A Novel Framework for the Operational Reliability Evaluation of Integrated Electric Power-Gas Networks

Osama Aslam Ansari, *Student Member, IEEE*, C. Y. Chung, *Fellow, IEEE*, and Enrico Zio, *Senior Member, IEEE*

***Abstract*—This paper proposes a new framework for the operational reliability evaluation of integrated electric power-gas networks (IEPGNs). First, a novel approach for modeling the failure modes of natural gas pipelines is presented. This approach utilizes the concept of virtual nodes and employs a gas release rate model to calculate the natural gas leaked from the pipelines. Thereafter, a four-state Markov model for natural gas-fired generators (NGFGs) with dual-fuel capabilities is proposed. The area risk method is then extended to include the proposed reliability models, and the partial reliability indices of the area risk method are evaluated using a non-sequential Monte Carlo simulation (NSMCS). A nonlinear optimization model is also proposed to calculate electric and gas load curtailments for each system state. This optimization model is linearized to obtain a mixed-integer linear programming (MILP) model for reducing the computational burden. The computational performance of NSMCS is further improved by adopting cross entropy (CE)-based importance sampling (IS). Finally, two test systems are employed to demonstrate the efficacy of the proposed framework. Case studies validate the importance of considering the proposed reliability models of IEPGNs for operational reliability evaluation. The impacts of operational strategies on the operational reliability indices are also demonstrated.**

***Index Terms*— Integrated electric power-gas networks, Monte Carlo simulation, operational reliability, reliability modeling.**

I. Introduction

THE penetration of natural gas-fired generators (NGFGs) in modern power systems has increased tremendously over the last decade owing to historically lower prices and the comparatively lower carbon intensity of natural gas [1]. Consequently, electric power systems and natural gas networks are becoming increasingly interdependent. This increased coupling poses considerable challenges to the reliable operation of integrated electric power-gas networks (IEPGNs). The impacts of component outages in one network can quickly propagate into the other, thereby jeopardizing the reliability of both networks [2]. Therefore, there is a heightened need to develop novel reliability evaluation tools to assist system operators in minimizing adequacy risks during the planning and operation of IEPGNs [3].

The existing literature on the reliability evaluation of IEPGNs can be broadly classified into two categories: long-term reliability evaluation and short-term, or operational reliability evaluation. In [4], the long-term reliability indices of IEPGNs are evaluated using a sequential Monte Carlo simulation (MCS) while considering power-to-gas and natural gas storage facilities. Reference [5] adopts reliability network equivalents to represent multi-state reliability models of IEPGN components and employs sequential MCS for reliability evaluation. The universal generating function technique is utilized in [6], where the multi-state models of gas injections to NGFGs are first calculated, followed by the reliability evaluation of power systems. In [7] and [8], the cascading effects of failures in IEPGNs are shown to decrease their long-term reliability. Reference [9] performs the reliability analysis of IEPGNs from the perspectives of system-level, customer-level, and resource analyses using non-sequential MCS (NSMCS). Although long-term reliability evaluation techniques are suitable for system planning purposes, operational reliability evaluation methods are required by system operators to schedule sufficient operating reserves to minimize adequacy risks in operational timescales [3].

A very limited number of frameworks have been proposed in the literature to assess the operational reliability of IEPGNs. In [10], the worst N-1 contingencies in distribution-level IEPGNs are considered, and a heuristic tree search algorithm is proposed to solve the load restoration optimization problem for calculating operational reliability indices. In a multi-energy system setting, [11] models the dynamic behavior of thermal loads and adopts sequential MCS for operational reliability assessment. In [12], the customers' ability to substitute energy sources to meet their energy demands is included in the operational reliability assessment of multi-energy systems.

Despite their worthy contributions, the existing frameworks for operational reliability evaluation of IEPGNs suffer three key drawbacks. First, the reliability models of natural gas networks are simplified. In particular, the existing studies incorporate only one mode of failures for natural gas pipelines, i.e., ruptures, while neglecting the two more dominant failure modes, which are pinholes and holes in the pipelines [13], [14]. Second, modern NGFGs are equipped with dual-fuel capabilities that allow them to switch between natural gas supply and an alternate fuel supply to generate power in the event of supply shortages [15], [16]. Such a process entails a

This work was supported in part by the Natural Sciences and Engineering Research Council (NSERC) of Canada and the Saskatchewan Power Corporation (SaskPower).

Osama Aslam Ansari, and C. Y. Chung are with the Department of Electrical and Computer Engineering, University of Saskatchewan, Saskatoon, SK, S7N 5A9, Canada (email: oa.ansari@usask.ca, c.y.chung@usask.ca).

Enrico Zio is with the Department of Energy, Politecnico di Milano, 20133 Milano, Italy, and also with the Centre de Recherche sur les Risques et les Crises (CRC), MINES ParisTech/PSL Université Paris, 75272 Paris, France, and also with the Department of Nuclear Engineering, Kyung Hee University, Seoul 02447, South Korea (e-mail: enrico.zio@polimi.it).

switching time, and probabilities are associated with the success and failure of this switching process. These characteristics of dual-fuel NGFGs (DF-NFGFs) are not considered in existing frameworks. Third, following outages in IEPGNs, different operational strategies are not considered when determining the minimum load curtailment. For instance, NGFGs are treated as low-priority, non-human need gas loads, and thus are curtailed first by natural gas system operators in the case of outages [17]. The first two drawbacks could result in underestimation, whereas the third drawback could lead to overestimation, of operational reliability indices of IEPGNs.

The purpose of this paper is therefore to extend the literature on operational reliability evaluation of IEPGNs by proposing a new framework that addresses the aforementioned limitations. A novel approach for reliability modeling of IEPGNs is first proposed that models all three failure modes of pipelines. To this end, a virtual node method is presented, and the natural gas released from the pipelines due to these failures is modeled. Additional probability distribution functions (PDFs) are defined to complete the reliability modeling of pipelines and consider the uncertainties of failure locations and diameters of leaks. Furthermore, a four-state Markov model for DF-NGFGs is proposed that considers the probabilities of successful and failed switching of fuel supply.

Thereafter, the area risk method [18] is extended to include the proposed reliability models of IEPGNs. The partial reliability indices of the area risk method are evaluated using a NSMCS. A new optimization model for evaluating the amounts of electric and gas load curtailments is, then, presented. This optimization model embeds the gas release rate model and allows the incorporation of different operational strategies by system operators. The original non-linear optimization model is linearized into a mixed-integer linear programming (MILP) model to reduce the computational burden of the proposed framework. Finally, to mitigate the low computational performance of NSMCS for evaluating operational reliability indices, importance sampling (IS) is adopted, whose parameters are obtained using cross entropy (CE) optimization [19]–[21].

The effectiveness of the proposed framework is demonstrated by its application to two test systems. The results clearly indicate the importance of including both the proposed reliability models of IEPGNs and the operational strategies of system operators. The good computational performance of the proposed framework is also shown in the case studies.

In summary, the main contributions of this work are:

1. A novel approach for comprehensive reliability modeling of IEPGNs is proposed. The approach allows for the thorough investigation of the impacts of multiple failure modes of pipelines and dual-fuel capabilities of DF-NGFGs on the operational reliability of IEPGNs.
2. A novel framework, based on the area risk method and NSMCS, is proposed to integrate the proposed reliability models for the evaluation of the operational reliability of IEPGNs. To analyze the system state, a new optimization model is also formulated, which is linearized to reduce the computational burden.
3. The CE-based IS technique is adopted to improve the computational efficiency of NSMCS in evaluating operational reliability indices.

The rest of the paper is organized as follows. Section II delineates the proposed approach for reliability modeling of IEPGNs. Section III describes the proposed framework for operational reliability evaluation of IEPGNs. Section IV discusses the results obtained from the selected case studies. Finally, Section V provides the conclusions of the work.

II. Reliability Model of IEPGNs

Consider a power system with N^{G} generators, N^{T} transmission lines, N^{B} buses, and N^{D} electric loads. Also, among N^{G} generators, let N^{NGFG} be the number of NGFGs. Also, consider a gas network with N^{W} gas wells or sources, N^{P} pipelines, N^{N} nodes, N^{L} gas loads, and N^{S} natural gas storage facilities. Various reliability models for the operational reliability evaluation of power systems exist in the literature, e.g., [18], [21]. Specifically, the generators and transmission lines of power systems are modelled using the following outage replacement rates (ORRs), which represent the probabilities of failure during the future lead time T:

$$ORR_g^{\mathrm{G}} = 1 - e^{-\lambda_g^{\mathrm{G}} T} \approx \lambda_g^{\mathrm{G}}\, T, \forall g \in \{1, \dots, N^{\mathrm{G}}\}, \quad (1)$$

$$ORR_l^{\mathrm{L}} = 1 - e^{-\lambda_l^{\mathrm{L}} T} \approx \lambda_l^{\mathrm{L}}\, T, \forall l \in \{1, \dots, N^{\mathrm{L}}\}, \quad (2)$$

where ORR_g^{G} and λ_g^{G} represent the ORR and failure rate of the gth generator, respectively, and ORR_l^{L} and λ_g^{G} represent the ORR and failure rate of the lth transmission line, respectively. Similar to power systems, also the gas sources and pipelines of gas networks can be modeled using ORRs:

$$ORR_w^{\mathrm{W}} = 1 - e^{-\lambda_w^{\mathrm{W}} T} \approx \lambda_w^{\mathrm{W}}\, T, \forall w \in \{1, \dots, N^{\mathrm{W}}\}, \quad (3)$$

$$ORR_p^{\mathrm{P}} = 1 - e^{-\lambda_p^{\mathrm{P}} T} \approx \lambda_p^{\mathrm{P}}\, T, \forall p \in \{1, \dots, N^{\mathrm{P}}\}. \quad (4)$$

In (3) and (4), ORR_w^{W} and λ_w^{W} describe the ORR and failure rate of the wth gas source, respectively, and ORR_p^{P} and λ_p^{P} describe the ORR and failure rate of the pth pipeline, respectively.

A. Reliability Model of Natural Gas Pipelines

In the event of unplanned failures, power systems and natural gas networks are operated in different manners. Whereas an outage of a transmission line in a power system results in the line being completely out of service, a pipeline in a natural gas network can still operate with reduced service after it suffers from a failure [13], [22]. Moreover, due to the slower dynamics of natural gas networks, the impacts of pipeline failures are more localized in gas networks than those of transmission lines' outages in power systems. Thus, it is important to extend the ORR model of pipelines in (4) to consider these characteristics of natural gas networks.

To realistically model the reduced service of pipelines, multiple failure modes of pipelines need to be considered. Typically, pipeline failures can be classified into three categories: 1) pinhole or crack, 2) hole and 3) rupture [13], [14]. These categories are differentiated based on the size of the leak in the pipeline. For a pinhole, the effective diameter of the leak is less than or equal to 0.02 m. If the effective diameter of the leak is greater than 0.02 m but less than the diameter of the pipeline, the leak is classified as a hole. Finally, for a rupture,

the effective diameter of the leak is greater than the pipeline diameter. Although a rupture causes a pipeline to be completely removed from service, a pipeline with a pinhole or a hole can operate with reduced service [23]. Note that the existing literature on the reliability evaluation of IEPGNs only considers ruptures, while completely neglecting the other failure modes. Moreover, the data from actual pipeline incidents indicate that ruptures only represent less than 16% of all pipeline failures, with pinhole and hole failures contributing 63.97% and 20.58%, respectively [13]. Thus, it seems relevant to consider also pinhole and hole failures, which are the dominant failure modes of pipelines, to realistically evaluate the operational reliability indices of IEPGNs. In what follows, a systematic approach is presented to incorporate all failure modes of pipelines for operational reliability evaluation.

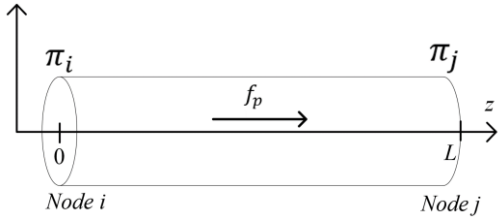

Fig. 1. A natural gas pipeline of length L between nodes i and j of a natural gas network under normal operating conditions.

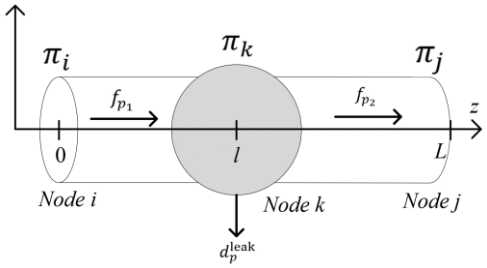

Fig. 2. The natural gas pipeline of Fig. 1 in which a pinhole or hole failure occurs at a distance ℓ from node i.

1) Virtual Node Approach

The rupture of a pipeline can be modeled by eliminating that specific pipeline from the gas network model. To model pinhole and hole failures, instead, a virtual node approach is here proposed. Consider Fig. 1, which represents the pth pipeline between nodes i and j of a gas network. In this figure, π_i and π_j represent the gas pressures at nodes i and j, respectively. f_p denotes the mass flow rate in the pipeline from node i to node j. Suppose a failure occurs at a distance ℓ from node i, which results in a leak. To model the natural gas released from this leak, a virtual node k is introduced at a distance ℓ from node i. As Fig. 2 shows, the gas released from this leak is modeled as an auxiliary gas load at this virtual node, which is represented by d_p^{leak}. This leak also modifies the original mass flow rate in the pipeline. Thus, f_p is replaced by two mass flow rates f_{p_1} and f_{p_2}. Although, this virtual node physically represents a pinhole or hole, it is treated as an additional node in the gas network model with its nodal pressure π_k. The nodal balance equation at this virtual node is given by:

$$f_{p_1} = f_{p_2} + d_p^{\text{leak}}, \tag{5}$$

where

$$f_{p_1}|f_{p_1}| = \psi_{p_1}^2(\pi_i^2 - \pi_k^2), \tag{6}$$

$$f_{p_2}|f_{p_2}| = \psi_{p_2}^2(\pi_k^2 - \pi_j^2). \tag{7}$$

In (6) and (7), ψ_{p_1} and ψ_{p_2} are constants for the Weymouth equation, and are calculated using the pipeline lengths ℓ and $L - \ell$, respectively.

To calculate the auxiliary load d_p^{leak} representing the gas released from leak in the pipeline, the following gas release rate model is adopted [23]:

$$d_p^{\text{leak}} = \alpha_p(1 + \beta_p \ell)^{-1/2}\sqrt{\pi_i}\,, \tag{8}$$

where α_p and β_p are constants given in Appendix A that depend on the diameter of the leak and pipeline parameters. Fig. 3 portrays the auxiliary load for varying distance and diameter of the leak on a 60-km pipeline with a 1 m diameter. This figure demonstrates that the gas released from the leak decreases as the distance from the starting node increases, and increases, as the diameter of the leak increases.

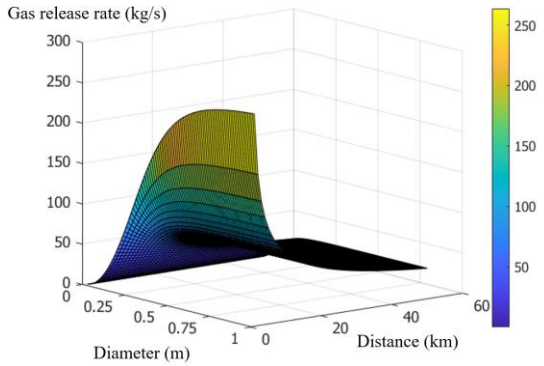

Fig. 3. Gas release rate from a leak of varying diameter and distance from the starting node on a 60-km gas pipeline.

2) PDFs for Pipelines Failures

Apart from the ORR for pipelines given by (4), additional PDFs are required to complete the reliability model of the pipelines, considering multiple failure modes. The following categorical PDF $\mathbb{f}_p(z)$ obtained from historical failure, data, models the type of failure for the generic pth pipeline,

$$\mathbb{f}_p(z) = \begin{cases} 0.6397 & z = 1 \\ 0.2058 & z = 2, \\ 0.1545 & z = 3 \end{cases} \tag{9}$$

where, $z = 1$, 2, and 3 denote pinhole, hole, and rupture failures, respectively. If the type of failure is a pinhole or hole, additional random variables need to be defined. For these types of failures, equation (8) and Fig. 3 show that the gas released from the leak depends on three factors: 1) the pressure at the starting node, 2) the distance of the leak from the starting node of the pipeline, and 3) the diameter of the leak. The pressure at the starting node is determined by solving the natural gas flow problem for gas networks or the combined power-gas flow problem for IEPGNs, as will be described later. The distance from the starting node and the diameter of the leak after failure occurrence need to be probabilistically modeled. In this work, a continuous PDF $\mathbb{f}_p^{loc}(\ell)$ is defined for the distance of the leak from the starting node. For the diameter, two continuous PDFs are defined - $\mathbb{f}_p^{\text{PH}}(\mathcal{d}_l)$ for pinhole and $\mathbb{f}_p^{\text{H}}(\mathcal{d}_l)$ for hole, where $\mathcal{d}_l$ represents the diameter of the leak. Based on the definitions of pinhole and hole given above, the domains of $\mathbb{f}_p^{\text{PH}}(\mathcal{d}_l)$ and $\mathbb{f}_p^{\text{H}}(\mathcal{d}_l)$ are $(0,0.02]$ and $(0.02, \mathcal{D}_p)$, respectively, where $\mathcal{D}_p$ is the diameter of the pth pipeline. The actual forms of these distributions are fitted on the available data. In this paper, for

the sake of simplicity, uniform distributions are assumed for $f_{loc}(\ell)$, $f_p^{\mathrm{PH}}(d_l)$ and $f_p^{\mathrm{H}}(d_l)$ over their respective domains.

B. Reliability Modeling of DF-NGFGs

As mentioned in the Introduction, modern NGFGs are equipped with dual-fuel capabilities that allow them to switch from natural gas supply to an alternative fuel supply. This switching action is taken in the event of natural gas supply shortages. For instance, during the "Bomb Cyclone" event in the U.S. that led to curtailments of natural gas supply, a 1,218 MW NGFG was able to switch to oil to continue producing electric power [15]. This switching process requires a fixed number of hours to complete, and it entails the risk of unsuccessful switching leading to the outage of the NGFG [17]. This behavior is similar to the operation of rapid-start natural gas generating units [18].

To model DF-NGFGs, a four-state Markov model is proposed in this paper, as depicted in Fig. 4. State 1 represents the normal operation mode of the DF-NGFG, where natural gas is used to produce electric power. State 2 represents the DF-NGFG outage. State 3 represents the operation of the DF-NGFG on alternate fuel. State 4 represents a temporary state, when the switching action fails. After the failure of switching, the DF-NGFG enters State 2 of outage. In Fig. 4, μ_{ij} denotes the transition rate from state i to state j.

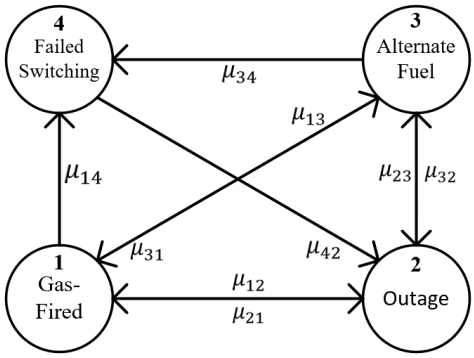

Fig. 4. Four-state Markov model for NGFGs with dual fuel capabilities.

III. Framework Proposed for The Operational Reliability Evaluation of IEPGNs

This section presents the framework proposed for the operational reliability evaluation of IEPGNs. The framework is founded on the area risk method [18] and NSMCS [24] and allows evaluating the operational reliability indices for a given lead time considering the previously proposed reliability models of natural gas pipelines and DF-NGFGs. The optimization model for evaluating electric and gas load curtailments considering the gas release rate model is also presented. In what follows, the proposed framework for evaluating the probabilities of electric load curtailment ($PELC$) and gas load curtailment ($PGLC$) for a given lead time T is explained.

A. Area Risk Method

The area risk method has been employed for operational reliability evaluation of power systems to consider rapid start generating units [18], wind generation [20], and energy storage. The area risk method splits the given lead time into several sub-periods, and the reliability indices in each sub-period are calculated. These reliability indices are, then, accumulated to obtain the operational reliability index for the given lead time. In this work, the area risk method is adopted to consider the switching time associated with the dual-fuel capabilities of DF-NGFGs.

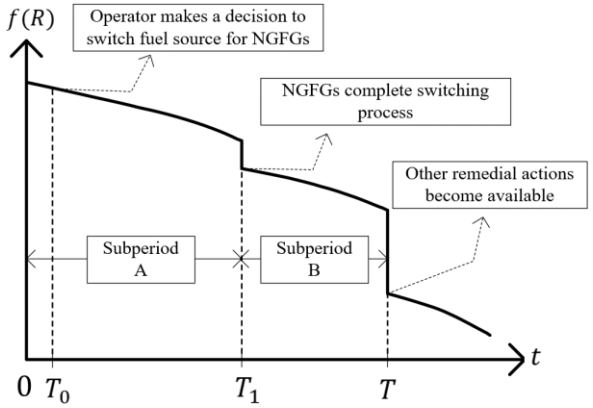

Fig. 5. The area risk method with NGFGs with dual-fuel capabilities

The area risk method is pictorially sketched in Fig. 5 for a lead time T. For subperiod A, i.e., from 0 to T_1, the $PELC$ and $PGLC$ are given by:

$$PELC_A = \int_0^{T_1^-} H_{\mathrm{Elect}}(\boldsymbol{x})\, f(\boldsymbol{x}) d\boldsymbol{x}\,, \tag{10}$$

$$PGLC_A = \int_0^{T_1^-} H_{\mathrm{Gas}}(\boldsymbol{x})\, f(\boldsymbol{x}) d\boldsymbol{x}\,, \tag{11}$$

where $H_{\mathrm{Elect}}(\cdot)$ and $H_{\mathrm{Gas}}(\cdot)$ are test functions, which will be defined later. $f(\cdot)$ is the combined PDF of the random variables in IEPGNs. Assuming that the outages of different components are independent of each other, $f(\cdot)$ can be expressed as:

$$f(\cdot) = f_{\mathrm{G}}(\cdot)\, f_{\mathrm{L}}(\cdot) f_{\mathrm{W}}(\cdot) f_{\mathrm{P}}(\cdot)\,, \tag{12}$$

where $f_{\mathrm{G}}(\cdot)$ and $f_{\mathrm{L}}(\cdot)$ represent the product of binomial distributions for the generators, and the product of Bernoulli distributions for the transmission lines, respectively. $f_{\mathrm{W}}(\cdot)$ denotes the product of binomial distributions for the natural gas sources. $f_{\mathrm{P}}(\cdot)$ represents the product of multiple PDFs for the natural gas pipelines, as defined in Section II.A. In subperiod A, the DF-NGFGs in IEPGNs are dependent on gas supply from the natural gas network to generate power. Therefore, the ORRs defined in (1) are used in $f_{\mathrm{G}}(\cdot)$ for DF-NGFGs.

Assuming that the system operator makes a decision at T_0 to switch the fuel supply for DG-NGFGs, the DG-NGFGs would complete the switching process at T_1, where $T_1 - T_0$ is the switching time for DG-NGFGs. After T_1, the DG-NGFGs that have been successfully switched, are no longer reliant on the natural gas network to generate power. Thus, they can still contribute to the power system if they are not in outage. Due to this switching action of DG-NGFGs, the evaluation of $PELC$ and $PGLC$ entail the calculation of two integrals:

$$PELC_B = \int_0^{T} H_{\mathrm{Elect}}(\boldsymbol{x})\, f(\boldsymbol{x}) d\boldsymbol{x} - \int_0^{T_1^+} H_{\mathrm{Elect}}(\boldsymbol{x})\, f(\boldsymbol{x}) d\boldsymbol{x}, \tag{13}$$

$$PGLC_B = \int_0^{T} H_{\mathrm{Gas}}(\boldsymbol{x})\, f(\boldsymbol{x}) d\boldsymbol{x} - \int_0^{T_1^+} H_{\mathrm{Gas}}(\boldsymbol{x})\, f(\boldsymbol{x}) d\boldsymbol{x}. \tag{14}$$

The first integral evaluates the indices at the end of subperiod B, whereas the second integral does it at the start of subperiod B. For this subperiod, the proposed four-state model for DF-NGFGs is employed instead of using ORRs. Specifically, given a vector of initial state probabilities $\boldsymbol{P}_0$ for the Markov model, the state probabilities of a DF-NGFG at a future lead time T_k can be evaluated by:

$$\boldsymbol{P}(T_k) = \boldsymbol{P}_0 \boldsymbol{P}_{\mathrm{S}}^{T_k/\Delta T}, \tag{15}$$

where $\boldsymbol{P}_{\mathrm{S}}$ is the discretized stochastic transition probability matrix and ΔT is the discretization time interval. The off-diagonal elements of $\boldsymbol{P}_{\mathrm{S}}$ are $\mu_{ij}\Delta T$, whereas the diagonal elements of $\boldsymbol{P}_S$ are $1-\sum_{j,i\neq j}\mu_{ij}\Delta T$. $\boldsymbol{P}(T)$ and $\boldsymbol{P}_0$ are then utilized to evaluate the first and second integrals, respectively. The total operational reliability indices for the given lead time are then given by:

$$PELC = PELC_A + PELC_B, \tag{16}$$

$$PGLC = PGLC_A + PGLC_B, \tag{17}$$

For simple cases, the integrals in (10), (11), (13), and (14) can be evaluated using analytical techniques, such as capacity outage probability tables [18]. For generality, in this paper, these integrals are estimated using NSMCS. In particular, by using NSMCS, any integral of the form $\int_0^{T_k} H_k(\boldsymbol{x})\, \mathbb{f}(\boldsymbol{x}) d\boldsymbol{x}$ can be estimated as:

$$\int_0^{T_k} H_k(\boldsymbol{x})\, \mathbb{f}(\boldsymbol{x}) d\boldsymbol{x} \approx \frac{1}{N_{\mathrm{S}}}\sum_{i=1}^{N_{\mathrm{S}}} H_k(\boldsymbol{x}_i)\,, \tag{18}$$

where N_{S} is the number of NSMCS samples drawn from $\mathbb{f}(\cdot)$.

B. Proposed Optimization Model for Minimum Load Curtailments

The two test functions in Section III.A are defined as follows:

$$H_{\mathrm{Elect}}(\boldsymbol{x}_i) = \begin{cases} 0 & S_{\mathrm{Elect}}(\boldsymbol{x}_i) - \sum_{j=1}^{N^{\mathrm{D}}} d_j \geq 0 \\ 1 & S_{\mathrm{Elect}}(\boldsymbol{x}_i) - \sum_{j=1}^{N^{\mathrm{D}}} d_j < 0 \end{cases}, \tag{19}$$

$$H_{\mathrm{Gas}}(\boldsymbol{x}_i) = \begin{cases} 0 & S_{\mathrm{Gas}}(\boldsymbol{x}_i) - \sum_{j=1}^{N^{\mathrm{L}}} l_j \geq 0 \\ 1 & S_{\mathrm{Gas}}(\boldsymbol{x}_i) - \sum_{j=1}^{N^{\mathrm{L}}} l_j < 0 \end{cases}. \tag{20}$$

In (19), d_j denotes the jth electric load demand and $S_{\mathrm{Elect}}(\cdot)$ is the sum of electric loads supplied in system state $\boldsymbol{x}_i$. Similarly, in (20), l_j denotes the jth gas load demand and $S_{\mathrm{Gas}}(\cdot)$ is the sum of gas loads supplied in system state $\boldsymbol{x}_i$.

To find $S_{\mathrm{Elect}}(\cdot)$ and $S_{\mathrm{Gas}}(\cdot)$, an optimization model is set up to determine the minimum values of the electric and gas loads curtailments. For this optimization model, the objective function is defined as:

$$\min \boldsymbol{\kappa}^{\mathrm{T}}\boldsymbol{r} + \boldsymbol{\lambda}^{\mathrm{T}}\boldsymbol{c}, \tag{21}$$

where $\boldsymbol{r} = \left[r_1, \dots, r_{N^{\mathrm{D}}}\right]^{\mathrm{T}}$ and $\boldsymbol{c} = \left[c_1, \dots, c_{N^{\mathrm{L}}}\right]^{\mathrm{T}}$ are vectors of the electric load and gas load curtailments, respectively. $\boldsymbol{\kappa}$, and $\boldsymbol{\lambda}$ denote the vectors for the electric load and gas load curtailment costs, respectively.

The constraints for power systems are as follows:

$$\boldsymbol{A}_{\mathrm{E}}\boldsymbol{g} - \boldsymbol{B}_{\mathrm{E}}\boldsymbol{d} + \boldsymbol{B}_{\mathrm{E}}\boldsymbol{r} = \boldsymbol{C}_{\mathrm{E}}\boldsymbol{p}\,, \tag{22}$$

$$p_i = \left(\theta_{from(i)} - \theta_{to(i)}\right)/x_i\,,\ \forall i \in \{1, \dots, N^{\mathrm{T}}\}, \tag{23}$$

$$0 \leq \boldsymbol{g} \leq \overline{\boldsymbol{g}}\,, \tag{24}$$

$$0 \leq \boldsymbol{r} \leq \boldsymbol{d}\,, \tag{25}$$

Equation (22) represents the nodal power balance constraints, where $\boldsymbol{g} = \left[g_1, \dots, g_{N^{\mathrm{G}}}\right]^{\mathrm{T}}$ and $\boldsymbol{d} = \left[d_1, \dots, d_{N^{\mathrm{D}}}\right]^{\mathrm{T}}$ represent the vectors of generators and electric load demands, respectively. $\boldsymbol{p} = \left[p_1, \dots, p_{N^{\mathrm{T}}}\right]^{\mathrm{T}}$ denotes the vector of power flows on the transmission lines. $\boldsymbol{A}_{\mathrm{E}}$, $\boldsymbol{B}_{\mathrm{E}}$, and $\boldsymbol{C}_{\mathrm{E}}$ are incidence matrices that model the connections of generators, electric loads, and transmission lines, respectively, to buses in the power system. The DC power flow model, which is formulated in terms of bus angles θ, is given by (23). Equations (24) and (25) set the limits on generator and electric load curtailments.

The constraints for the gas network are described as follows:

$$\boldsymbol{A}_{\mathrm{G}}\boldsymbol{w} - \boldsymbol{B}_{\mathrm{G}}\boldsymbol{l} + \boldsymbol{B}_{\mathrm{G}}\boldsymbol{c} + \boldsymbol{D}_{\mathrm{G}}\boldsymbol{s}_{\mathrm{dch}} - \boldsymbol{D}_{\mathrm{G}}\boldsymbol{s}_{\mathrm{ch}} - \boldsymbol{E}_{\mathrm{G}}\boldsymbol{n} = \boldsymbol{C}_{\mathrm{G}}\boldsymbol{f}\,, \tag{26}$$

$$f_p\left|f_p\right| = \psi_p^2\left(\Pi_{from(p)} - \Pi_{to(p)}\right),\ \forall p \in \{1, \dots, N^{\mathrm{P}}\}, \tag{27}$$

$$\boldsymbol{m}_{\mathrm{s}} - \boldsymbol{s}_{\mathrm{dch}}\Delta T + \boldsymbol{s}_{\mathrm{ch}}\Delta T = \boldsymbol{0}, \tag{28}$$

$$d_p^{\mathrm{leak}} = \alpha_p\left(1+\beta_p l\right)^{-1/2}\sqrt{\pi_i}\,,\ \forall p \in \Omega_{leak} \tag{29}$$

$$\underline{\boldsymbol{\Pi}} \leq \boldsymbol{\Pi} \leq \overline{\boldsymbol{\Pi}}, \tag{30}$$

$$\underline{\boldsymbol{f}} \leq \boldsymbol{f} \leq \overline{\boldsymbol{f}}, \tag{31}$$

$$\boldsymbol{0} \leq \boldsymbol{c} \leq \boldsymbol{l}, \tag{32}$$

$$\boldsymbol{0} \leq \boldsymbol{s}_{\mathrm{dch}} \leq \overline{\boldsymbol{s}}_{\mathrm{dch}},\ \boldsymbol{0} \leq \boldsymbol{s}_{\mathrm{ch}} \leq \overline{\boldsymbol{s}}_{\mathrm{ch}}. \tag{33}$$

Equation (26) represents the nodal balance equation for the gas network, where $\boldsymbol{w} = \left[w_1, \dots, w_{N^{\mathrm{W}}}\right]^{\mathrm{T}}$ and $\boldsymbol{l} = \left[l_1, \dots, l_{N^{\mathrm{L}}}\right]^{\mathrm{T}}$, represent the vectors of gas sources and gas load demands, respectively. $\boldsymbol{s}_{\mathrm{dch}} = \left[s_1^{\mathrm{dch}}, \dots, s_{N^{\mathrm{S}}}^{\mathrm{dch}}\right]^{\mathrm{T}}$ and $\boldsymbol{s}_{\mathrm{ch}} = \left[s_1^{\mathrm{ch}}, \dots, s_{N^{\mathrm{S}}}^{\mathrm{ch}}\right]^{\mathrm{T}}$ are vectors of discharge and charge mass flow rates, respectively, for gas storage facilities. $\boldsymbol{n} = \left[n_1, \dots, n_{N^{\mathrm{NGFG}}}\right]^{\mathrm{T}}$ is a vector of NGFG gas consumptions. $\boldsymbol{f}$ is a vector of gas flows in the pipelines. Similar to power systems, $\boldsymbol{A}_{\mathrm{G}}$, $\boldsymbol{B}_{\mathrm{G}}$, $\boldsymbol{C}_{\mathrm{G}}$, $\boldsymbol{D}_{\mathrm{G}}$, and $\boldsymbol{E}_{\mathrm{G}}$ are incidence matrices, which denote the connections of gas sources, gas loads, pipelines, gas storages, and NGFGs, respectively, to nodes in the gas network. The Weymouth equations of the pipeline, which are formulated in terms of squared nodal pressure Π, are given by (27). The state-of-charge of gas storage facilities is modeled by (28). Equation (29) models the auxiliary load by using the gas release rate model, as described in Section II.A for the set of pipelines with failures Ω_{leak}. Equations (30) – (33) represent the limits on gas network variables. Note that the matrices $\boldsymbol{A}_{\mathrm{G}}$, $\boldsymbol{B}_{\mathrm{G}}$, $\boldsymbol{C}_{\mathrm{G}}$, $\boldsymbol{D}_{\mathrm{G}}$, and $\boldsymbol{E}_{\mathrm{G}}$ are modified when the cardinality of Ω_{leak} is greater than zero to include virtual nodes.

The constraints coupling the power system and gas network are given by:

$$n_i = \tau_i g_i,\ \forall i \in \Omega_{\mathrm{NGFG}}\,, \tag{34}$$

where τ_i is a constant representing the power conversion factor of the ith NGFG, and Ω_{NGFG} is the set of NGFGs. This set contains both conventional NGFGs and DF-NGFGs. It is modified depending on whether the DF-NGFGs are operating on natural gas supply or alternate fuel.

The optimization model given by (21) – (34) is nonlinear due to the inclusion of the gas release rate model and Weymouth equations. Nonlinear optimization models incur a large computational burden and therefore cannot be directly employed for operational reliability assessment. In this paper, the nonlinear gas release rate model is linearized using a piecewise linearization method as given in Appendix B. After linearization, the optimization model is reduced to a MILP model.

C. CE-IS based NSMCS

The traditional NSMCS incurs a large computational burden when the values of $PELC$ and $PGLC$ being estimated are small. This is the case for operational reliability evaluation of IEPGNs. Therefore, in this paper, the widely used IS technique [24] is adopted to reduce the computational time. Using IS, the integral in (18) is evaluated using the following estimator:

$$\int_0^{T_k} H_k(\boldsymbol{x})\, \mathbb{f}(\boldsymbol{x}) d\boldsymbol{x} = \frac{1}{N_{\mathrm{S}}}\sum_{i=1}^{N_{\mathrm{S}}} H_k(\boldsymbol{x}_i)\mathbb{f}(\boldsymbol{x}_i)/\mathbb{f}^*(\boldsymbol{x}_i)\,, \tag{35}$$

where the samples are now drawn from $\mathbb{f}^*(\cdot)$, which is called the IS density. In this paper, the parameters of the IS density are

obtained using the CE optimization. Interested readers are referred to [19]–[21] for a detailed explanation of CE-IS based NSCMS.

IV. Simulation Results

This section presents the key results obtained with the proposed framework. The simulations are performed on two test systems: 1) *Test System A*, which comprises the 6-bus power system integrated with the 7-node gas network [25] (Fig. 6), and 2) *Test System B*, which comprises the 24-bus IEEE reliability test system (RTS) [26] integrated with the 20-node Belgian gas network [27] (Fig.7). The additional data, including failure rates, and the parameters of the CE-IS-based NSMCS, are provided in [28]. For NSMCS, the coefficient of variation of $PGLC$ is selected and the stopping criterion is set to 5%. All simulations are run on a PC with a 3.40 GHz Intel® Core i7-6700 CPU and 16 GB of RAM. The proposed framework is implemented in MATLAB 2019 and the GUROBI 9.0.1 solver is used to solve the optimization problem.

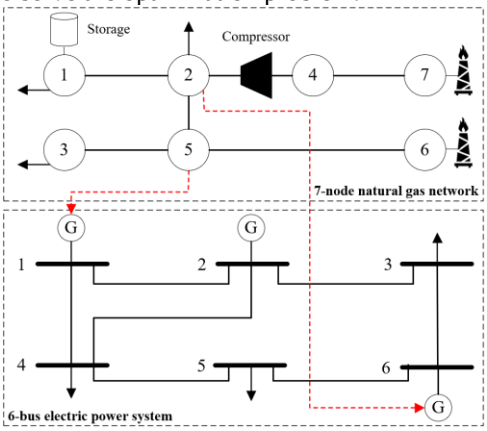

Fig. 6. *Test System A* comprising a 6-bus power system and a 7-node gas network

A. Demonstrative Cases

To demonstrate the importance of performing operational reliability assessment for IEPGNs, two cases are considered. In *Case A*, *Test System A* is decoupled. In *Case B*, the electric and gas networks of *Test System A* are coupled via NGFGs. For both cases, the total electric and gas load demands are set to 270 MW and 32.09 kg/s, respectively. The lead time is set to 2 hours.

Table I compares the $PELC$ and $PGLC$ indices for the two cases. The results show that the operational reliabilities of individual networks are lower for *Case B* than for *Case A*. The lower $PELC$ for *Case A* is attributed to the supply of natural gas to NGFGs being significantly constrained in the event of pipeline outages. In particular, two pipelines connecting gas sources to other nodes in the gas network are crucial to maintain the supply of natural gas to NGFGs. Similarly, the $PGLC$ in *Case B* is ~10% higher than in *Case A*. This is because the gas demands of NGFGs are not included in *Case A* and, thus, the probability of natural gas loads being supplied due to the absence of NGFG gas demands is higher. Also, for both cases, the $PGLC$ is lower than the $PELC$ due to higher reliabilities of individual gas sources and pipelines. To sum up, the results show that the need to consider the interactions between electric and gas networks to accurately evaluate the operational reliability indices of these networks.

The computational performance of the operational reliability evaluation framework is critical to facilitate its application during real system operation. Table I shows that the computational performance of the proposed method is clearly several orders of magnitude higher than that of traditional NSMCS.

TABLE I
PELC and PGLC of IEPGNs For Two Demonstrative Cases

Method	Indices	*Case A*	*Case B*	% Difference
Proposed	$PELC$ ($\times 10^{-3}$)	6.570	9.039	37.57
	$PGLC$ ($\times 10^{-4}$)	8.785	9.733	10.79
	Time (s)	562.92	404.87	-
Traditional NSMC	$PELC$ ($\times 10^{-3}$)	6.488	9.124	40.62
	$PGLC$ ($\times 10^{-4}$)	8.726	9.757	11.81
	Time (s)	215,892	151,333	-

B. Impact of Failures of Natural Gas Pipelines

In this subsection, we demonstrate the efficacy of the proposed reliability model of natural gas pipelines. Two case studies are performed. In *Case C*, only gas pipeline ruptures are taken into account; whereas in *Case D*, the proposed reliability model is adopted to consider all three failure modes of gas pipelines.

Table II shows the $PELC$ and $PGLC$ indices for varying values of total natural gas load demands and lead times. From the Table, it can be deduced that the $PELC$ and $PGLC$ indices

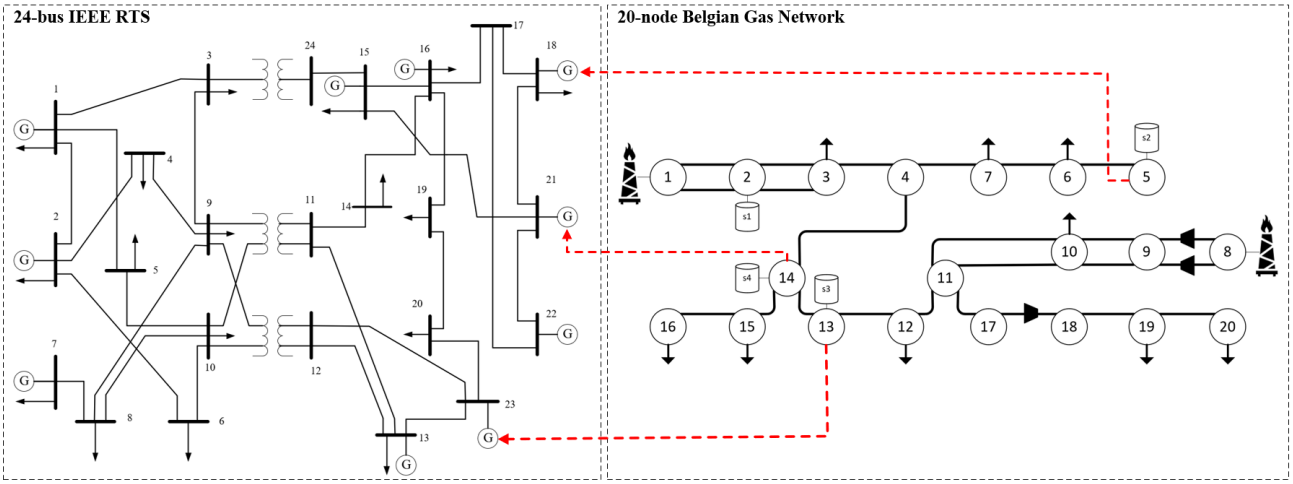

Fig. 7. *Test System B* comprising the 24-bus IEEE RTS and the 20-node Belgian Gas Network

TABLE II
OPERATIONAL RELIABILITY INDICES FOR VARYING GAS LOADS AND LEAD TIMES

Increase in Gas Load		-10%		0%		10%		20%		30%	
Case	Lead Time (h)	PELC ($\times 10^{-3}$)	PGLC ($\times 10^{-3}$)	PELC ($\times 10^{-3}$)	PGLC ($\times 10^{-3}$)	PELC ($\times 10^{-3}$)	PGLC ($\times 10^{-3}$)	PELC ($\times 10^{-3}$)	PGLC ($\times 10^{-3}$)	PELC ($\times 10^{-3}$)	PGLC ($\times 10^{-3}$)
Case C	1	4.814	2.508	5.067	2.598	5.270	2.531	6.731	2.531	6.731	3.465
	2	9.183	4.801	9.666	4.975	10.053	5.270	12.085	5.269	12.085	7.484
	3	14.394	6.864	14.941	7.109	15.511	7.671	19.397	7.666	19.397	10.985
	4	20.047	9.276	21.751	9.624	22.044	10.345	25.992	10.335	25.992	14.339
Case D	1	4.353	0.268	4.291	0.262	4.595	0.283	5.416	0.303	5.199	1.709
	2	8.954	0.864	9.039	0.973	9.001	0.981	10.928	1.021	11.771	3.482
	3	12.569	1.155	14.174	1.157	1.264	1.351	15.966	1.478	17.041	5.216
	4	17.772	1.732	19.424	1.881	19.192	2.015	23.323	2.430	22.741	6.514

are overestimated in *Case C*. When all three failure modes of pipelines are treated in *Case D*, the $PELC$ and $PGLC$ indices are lower. With pinhole and hole failure modes, which are the two dominant failure modes of pipelines, the pipelines can be operated with reduced service, which still allows the gas network to supply gas load demands to both the gas network and NGFGs in the power system. This leads to improved operational reliability of the gas network and power system. Table II also indicates that, as expected, this difference is higher for the gas network, i.e., the operational reliability of the gas network is more significantly improved than that of the power system. Furthermore, this improvement in the operational reliability of the gas network is greater at higher gas loads.

C. Impacts of DF-NGFGs

The impacts of DF-NGFGs on the operational reliability of IEPGNs are analyzed below. Two case studies are performed. In *Case E*, the DF-NGFGs are not modeled and are treated as conventional NGFGs. In *Case F*, the proposed reliability model of DF-NGFGs is considered. For both cases, the total lead time is set to 3 hours. For *Case F*, the switching time of DF-NGFGs is set to 2 hours, and T_0 in Fig. 5 is set to 10 minutes.

Table III provides the results for the two case studies. The dual-fuel switching capabilities of DF-NGFGs clearly improve the operational reliability of IEPGNs. As the switching process for DF-NGFGs completes in Subperiod B, these NGFGs are no longer constrained by the supply of gas from the gas network, thus shielding the power system from the impacts of gas network outages. The switching action of DF-NGFGs also slightly improves the reliability of the gas network, as the total amount of gas load being served is reduced.

TABLE III
OPERATIONAL RELIABILITY INDICES WITH DF-NGFGS

Case	Indices	Subperiod A	Subperiod B	Total
Case E	$PELC$ ($\times 10^{-3}$)	9.039	5.135	14.174
	$PGLC$ ($\times 10^{-4}$)	9.733	1.840	11.573
Case F	$PELC$ ($\times 10^{-3}$)	9.039	4.128	13.168
	$PGLC$ ($\times 10^{-4}$)	9.733	1.688	11.421

D. Practical Considerations

In the optimization model of Section III.B, the values of $\boldsymbol{\kappa}$ and $\boldsymbol{\lambda}$ significantly impact the amounts of electric and gas load curtailments and, thus, affect the operational reliability indices. In this work, three practical strategies are considered. In *Strategy 1*, the electric and gas loads are assumed to have equal priority, i.e., the per-unit electric and gas load curtailment costs are equal. In *Strategy 2*, the gas loads of gas networks have higher priority than the gas loads of NGFGs. In *Strategy 3*, the gas storage facilities in gas networks are only used to supply gas network loads. The lead time is set to 3 hours.

Table IV compares the results for the three operational strategies. As expected, the operational reliability of the electric power system is highest for *Strategy 1* and lowest for *Strategy 3*. On the contrary, the operational reliability of the gas network is highest for *Strategy 3* and lowest for *Strategy 1*. In *Strategy 2*, the gas loads of NGFGs are considered as low priority loads and therefore are curtailed first, leading to reduced reliability of the power system. *Strategy 3* indicates that electric power system operators need to acquire access to gas storage facilities to improve the operational reliability of their networks. This is because these storage facilities are primarily developed to serve the non-electric gas load demands of the gas network.

TABLE IV
OPERATIONAL RELIABILITY INDICES CONSIDERING DIFFERENT OPERATIONAL STRATEGIES

Strategy	Indices	
Strategy 1	$PELC$ ($\times 10^{-3}$)	14.174
	$PGLC$ ($\times 10^{-3}$)	1.157
Strategy 2	$PELC$ ($\times 10^{-3}$)	15.307
	$PGLC$ ($\times 10^{-3}$)	1.133
Strategy 3	$PELC$ ($\times 10^{-3}$)	16.301
	$PGLC$ ($\times 10^{-3}$)	1.041

E. Case Studies for Test System B

TABLE V
OPERATIONAL RELIABILITY INDICES FOR TEST SYSTEM B

Indices	*Case A*	*Case B*	*Case C*	*Case D*
$PELC$ ($\times 10^{-5}$)	3.328	3.860	10.207	9.696
$PGLC$ ($\times 10^{-6}$)	2.943	3.178	8.531	4.225
Time (s)	3,549.1	2,851.6	2,054.1	2,687.5
Indices	*Case E*	*Case F*	*Strategy 2*	*Strategy 3*
$PELC$ ($\times 10^{-5}$)	9.696	9.221	10.471	10.859
$PGLC$ ($\times 10^{-6}$)	4.225	4.203	3.975	3.802
Time (s)	2,687.5	2,889	2,456.8	2,994.7

In this subsection, we perform case studies on *Test System B* to show the scalability of the proposed framework. The results are shown in Table V. For *Cases A* and *B*, the lead time is two hours; for the rest, the lead time is 3 hours. Generally, the operational reliability of *Test System B* is higher than that of *Test System A*, due to the presence of multiple generating units in each generation station and redundant components in the gas network. The computational burden for this test system is expectedly higher than that of *Test System A*. The difference between the indices of *Cases C* and *D* reiterate the importance of considering all failure modes of the pipelines. The results presented in Table V also reinforce the importance of considering the dual-fuel capabilities of DF-NFGFs for the operational reliability evaluation of IEPGNs and the impacts of operational strategies on the reliability indices.

V. Conclusion

This paper proposes a novel framework for operational reliability evaluation of IEPGNs. Such framework includes a detailed reliability model of natural gas pipelines for realistically calculating reliability indices. It also accounts for the dual-fuel capabilities of DF-NGFGs, that are shown to improve the operational reliability of IEPGNs. The linear formulation of the proposed optimization model and the adoption of CE-based IS ensure high computational efficiency and make it feasible to adopt the proposed framework in practice. The results on the test cases analyzed indicate that the operational reliability indices of IPEGNs are improved when all three failure modes of pipelines are considered. In addition, the impacts of dual-fuel capabilities of DF-NGFGs and different operational strategies of system operators on operational reliability indices are demonstrated.

Appendix A

The coefficients of the gas release rate model in (8) are given as follows [23]:

$$\alpha_p = \frac{\pi \mathcal{D}_p^2 \sigma_p}{4} \sqrt{\gamma \rho_0 \left(\frac{2}{\gamma+1}\right)^{(\gamma+1)(\gamma-1)}} \tag{36}$$

$$\beta_p = \left(4\sigma^2 \zeta_p / d_p\right)(2/(\gamma+1))^{2/(\gamma-1)}. \tag{37}$$

In (1) and (2), $\mathcal{D}_p$ and ζ_p represent the diameter and friction factor of the pth pipeline, respectively. γ and ρ_0 are the specific heat ratio and density of natural gas at operating conditions, respectively. σ models the ratio of the effective hole area to the cross-sectional area of the pipeline, or,

$$\sigma = \omega d_l^2 / \mathcal{D}_p^2, \tag{38}$$

where d_l is the diameter of the leak and ω is a constant modeling the irregular shape of the leak.

Appendix B

Let $\hbar(y)$ be a non-linear function of y, then using the incremental model, $\hbar(y)$ is linearized as

$$\hbar(y) = \hbar(y_1) + \sum_{i=1}^{P} \left(\hbar(y_{i+1}) - \hbar(y_i)\right)\delta_i \tag{39}$$

$$y = y_1 + \sum_{i=1}^{P} (y_{i+1} - y_i)\delta_i \tag{40}$$

$$\delta_{i+1} \le \alpha_i,\ \alpha_i \le \delta_i\ \forall i \in \{1, .., P-1\} \tag{41}$$

$$0 \le \delta_i \le 1,\ \forall i \in \{1, \dots, P\} \tag{42}$$

where P is the number of points for linearization and α is a binary variable.

VI. References

[1] International Energy Agency (IEA), "Natural gas-fired power," *IEA*, Paris, France, 2020. [Online]. Available at: https://www.iea.org/reports/natural-gas-fired-power

[2] North American Electric Reliability Corporation (NERC), "Special reliability assessment: Potential bulk power system impacts due to severe disruptions on the natural gas system," *NERC*, Atlanta, GA, USA, Nov. 2017.

[3] NERC, "Short-term special assessment: Operational risk assessment with high penetration of natural gas-fired generation," *NERC*, Atlanta, GA, USA, May 2016.

[4] Z. Zeng, T. Ding, X. Xu, Y. Yang, and Z. Dong, "Reliability evaluation for integrated power-gas systems with power-to-gas and gas storages," *IEEE Trans. Power Syst*., vol. 35, no. 1, pp. 571-583, Jan. 2020.

[5] S. Wang, Y. Ding, C. Ye, and C. Wan, "Reliability evaluation of integrated electricity-gas system utilizing network equivalent and integrated optimal power flow techniques," *J. Mod. Power Syst. Clean Energy*, vol. 7, no. 6, pp. 1523-1535, Nov. 2019.

[6] M. Bao, Y. Ding, C. Singh, and C. Shao, "A multi-state model for reliability assessment of integrated gas and power systems utilizing universal generating function techniques," *IEEE Trans. Smart Grid*, vol. 10, no. 6, pp. 6271-6283, Nov. 2019.

[7] M. Bao, Y. Ding, C. Shao, Y. Yang, and P. Wang, "Nodal reliability evaluation of interdependent gas and power systems considering cascading effects," *IEEE Trans. Smart Grid*, vol. 11, no. 5, pp. 4090-4104, Sep. 2020.

[8] Z. Bao, Z. Jiang, and L. Wu, "Evaluation of bi-directional cascading failure propagation in integrated electricity-natural gas system," *Int. J. Elect. Power and Energy Syst*., vol. 121, Oct. 2020.

[9] H. Su, E. Zio, et al., "A systematic method for the analysis of energy supply reliability in complex integrated energy systems considering uncertainties of renewable energies, demands and operations," *J. Cleaner Production*, vol 267, Sep. 2020.

[10] Y. Liu, Y. Su, Y. Xiang, J. Liu, L. Wang, and W. Wu, "Operational reliability assessment for gas-electric integrated distribution feeders," *IEEE Trans. Smart Grid*, vol. 10, no. 1, pp. 1091-1100, Jan. 2019.

[11] M. H. Shariatkhah, M. R. Haghifam, M. Parsa-Moghaddam, and P. Siano, "Modeling the reliability of multi-carrier energy systems considering dynamic behavior of thermal loads," *Energy and Buildings*, vol. 103, pp. 375-383, Sep. 2015.

[12] S. Wang, C. Shao, Y. Ding, and J. Yan, "Operational reliability of multi-energy customers considering service-based self-scheduling," *Applied Energy*, vol. 254, Nov. 2019.

[13] European Gas Pipeline Incident Data Group (EGIG), "10th report of the European Gas Pipeline Incident Data Group (period 1970-2016)," *EGIG*, Groningen, Netherlands, Publication No. VA 17.R.0395, Mar. 2018.

[14] H. Su, J. Zhang, E. Zio, N. Yang, X. Li, and Z. Zhang, "An integrated systemic method for supply reliability assessment of natural gas pipeline networks," *Applied Energy*, vol. 209, pp. 489-501, Jan. 2018.

[15] U.S. Energy Information Administration (EIA), "Natural gas-burning power plant operations vary during periods of cold weather," *U.S. EIA*, Jan. 2019. Accessed Sep. 25, 2020. [Online]. Available: https://www.eia.gov/todayinenergy/detail.php?id=37992#tab1

[16] X. Zhang, M. Shahidehpour, A. Alabdulwahab, and A. Abusorrah, "Security-constrained co-optimization planning of electricity and natural gas transportation infrastructures," *IEEE Trans. Power Syst.*, vol. 30, no. 6, pp. 2984-2993, Nov. 2015.

[17] NERC, "2013 special reliability assessment: Accommodating an increased dependence on natural gas for electric power: Phase-II: A vulnerability and scenario assessment for the North American bulk power system," *NERC*, Atlanta, GA, USA, May 2013.

[18] R. Billinton and R. N. Allan, *Reliability Evaluation of Power Systems*, 2nd ed. New York, NY, USA: Plenum, 1996.

[19] R. Y. Rubinstein and D. P. Kroese, *The Cross-Entropy Method*, 1st ed., New York, NY, USA: Springer, 2004.

[20] O. A. Ansari, and C. Y. Chung, "A hybrid framework for short-term risk assessment of wind-integrated composite power systems," *IEEE Trans. Power Syst.*, vol. 34, no. 3, pp. 2334-2344, May 2019.

[21] O. A. Ansari, Y. Gong, W. Liu, and C. Y. Chung, "Data-driven operation risk assessment of wind-integrated power systems via mixture models and importance sampling," *J. Modern Power Syst. Clean Energy*, vol. 8, no. 3, pp. 437-445, May 2020.

[22] Z. Han, and G. W. Weng, "An overview of quantitative risk analysis methods for natural gas pipelines," *J. China Safety Science*, vol. 19, pp. 154-164, Jan. 2009.

[23] Y-D. Jo, and D. A. Crowl, "Individual risk analysis of high-pressure natural pipelines," *J. Loss Prevention in the Process Industries*, vol. 21, no. 6, pp. 589-595, Nov. 2008.

[24] E. Zio, *The Monte Carlo Simulation Method for System Reliability and Risk Analysis*, 1st ed., London, UK: Springer, 2013.

[25] C. Liu, M. Shahidehpour, Y. Fu, and Z. Li, "Security-constrained unit commitment with natural gas transmission constraints," *IEEE Trans. Power Syst*., vol. 24, no. 3, pp. 1523-1536, Aug. 2009.

[26] Reliability Test System Task Force of the IEEE Subcommittee on the Application of Probability Methods, "IEEE reliability test system," *IEEE Trans. Power App. Syst*., vol. 1, pp. 2047-2054, 1979.

[27] D. De Wolf, and Y. Smeers, "The gas transmission problem solved by an extension of the simplex algorithm," *Management Science*, vol. 46, no. 11, pp. 1454-1465, Nov. 2000.

[28] O. A. Ansari, "Additional Data IEPGNs," [Online]. Available at: https://oaansari.com/files/Additional_Data_IEPGNs.pdf